2

Air cushion theory

2.1 Introduction

Development of air cushion theory is closely related to the development of hovercraft themselves, particularly of flexible skirts.

Early air cushion vehicles were conceived with the object of drag reduction for a marine craft. The concept used was air lubrication of the wet hull surface. From practical experience with high-speed stepped hull planing boats in the early part of this century, it was realized that air lubrication did reduce the water friction; however, it was difficult to reduce wave-making resistance. For this reason, the concept of injecting lubricating air over the wetted surface was replaced by use of a thicker air cushion.

In China, this theory was put into effect as a plenum chamber hovercraft with thin 'sidewalls' at the edge of the cushion, the hovercraft '33', built at the Harbin Shipbuilding Engineering Institute (HSEI) in 1958. The air clearance under the sidewalls was very small, so it 'skated' over the water or ground and it is difficult to say that this craft had real amphibious qualities.

Sir Christopher Cockerell invented the principle of the peripheral jet hovercraft, whereby the air cushion was fed with air and also maintained by means of air flow momentum change at a high-velocity peripheral air curtain. Air cushion efficiency (depth of air cushion and thus obstacle clearance) was enhanced several times compared with that of the plenum chamber hovercraft fed with air directly into the cushion. Even so, prototype craft barely had amphibious ability. The Saunders Roe SR.N1 weighing 3.4 t, with an air clearance of approximately 200 mm, could only operate on smooth surfaces such as concrete, level beach or smooth water. The initial principles were nevertheless proved and a test bed made available for further development.

In practical terms, the amphibious capability of the SR.N1 was almost non-existent. It required another technological leap before the concept could be used for practical purposes. Nevertheless, the various theories to explain the peripheral jetted hovercraft were enthusiastically followed up in the 1960s by the scientific community. These include thin jet theory, thick jet theory, jet equilibrium theory and the various research efforts to understand the effect of different cushion plan-forms and compartmentation.

Flexible skirts to contain and deepen the cushion were the key idea needed to step forward. This concept began its development on hovercraft such as the SR.N1 as

flexible extensions to the air jet nozzles. These skirts significantly enhanced the obstacle clearance, giving real capability in a seaway as well as over rough ground and truly demonstrated amphibious capabilities.

The necessary condition for a hovercraft with peripheral jets to take off from static hovering to planing is that the air clearance of such a craft is at least larger than 0.5–0.8 times the depression caused by the cushion pressure on the water surface. If the hover gap is less than this, the hard structure will interact with the induced waves as the craft accelerates, greatly increasing the drag. However, for a hovercraft with flexible skirts the air gap underneath the skirt itself is not a key condition for the take-off of the craft, since the skirts will deform under the action of the induced wave-form.

The flexible skirted ACV is easier to accelerate through hump speed in rough water as well as over calm water for the same reasons – the skirt deforms under the action of the water surface. Nevertheless the power needed to traverse the drag peak (or 'hump') between the displacement and the planing condition is relatively high for a jetted skirt.

Engineers looked at different concepts of cushion geometry and skirts (see Chapter 7) to reduce the drag. Jet extensions gave way to bag skirts with smaller jet extensions and eventually the jet extensions were replaced with convolutions called fingers by the end of the 1960s (see Fig. 2.3). Thus, although the actual air clearance decreased because of the lower air cushion efficiency of such skirt types, the effective cushion depth greatly increased and both drag and required power were reduced.

The bag and finger type skirt has had great vitality, its design evolving continuously from the mid 1960s to the present, with gradually improving resistance characteristics and responsiveness, improving ride quality over rough surfaces. To date specific lift power has decreased to 14.7–19.4 kW/t (20–25 shp/t) for current craft compared with 73 kW/t (100 shp/t) for early ACVs (SR.N1), i.e. a factor of five, due to decreasing air clearance requirements beneath the flexible skirt.

At the present stage of development of ACVs and SES, the problems with respect to take-off from displacement mode to planing mode are no longer a key technical issue. Rather, the flexible skirt should be designed to meet the designer's seaworthiness requirements. In this respect, the concept of wave pumping has been identified as an important issue (the physical concept will be described later in this chapter) and designers consequently pay more attention to pitch and heave damping characteristics.

It may safely be taken for granted from this that it is better for designers to determine the lift power according to non-dimensional flow rate rather than relative air gap. It is also more convenient and reasonable to calculate lift power according to non-dimensional flow rate. The air gap is not a unique criterion for deciding the air cushion performance of craft; however, by experience, one still can use the air gap as one measure for assessing the air cushion performance.

Static air cushion theories derived in the 1960s are still suitable for describing the powering performance of craft with modern flexible skirt designs and so these are summarized below. The text in this chapter will proceed with air cushion theory from early research; then the flow rate coefficient method; the wave-pumping concept and its requirements; the determination of the heaving damping coefficient and finally the heave stability derivatives of ACVs.

2.2 Early air cushion theory developments

Although the theories mentioned below may seem to be out of date, it is useful to study them in order to understand the air cushion rationale. While peripheral air jets are no longer used in practice, the basic understanding developed through these theories is still equally valid for modern ACVs.

Theory of thin peripheral jet air cushion hovering on a rigid surface

This theory was used on early ACVs with rigid jet nozzles over ground for determining the air cushion performance. It assumes that:

- The nozzles are infinitely thin, therefore the air flow is jetted uniformly perpendicular to the centre line of the jet.
- The air flow jetted from nozzles is non-viscous and incompressible.
- The air flow jetted from nozzles will not combine with media around the air jet (induced flows are not treated).
- The cushion is supported on a rigid surface.

The transverse section of such an ACV is shown in Fig. 2.1. According to the theory for flow momentum,

$$hp_c = \rho_a V_j^2 t\,(1 + \cos\theta) = \rho_a V_j^2 xh \tag{2.1}$$

where p_c is the cushion pressure (N/m^2), ρ_a the air density (Ns^2/m^4), t the width of nozzle (m), h the air clearance (m), V_j the mean velocity of jets (m/s), θ the angle between the centre-line of the nozzle and the craft baseline (°) and

$$x = (1 + \cos\theta)t/h$$

Then the total pressure of the jet can be expressed as

$$P_t = 0.5\rho_a V_j^2 + fp_c \tag{2.2}$$

where P_t is the total pressure of the jet at the nozzle (N/m^2) and f the coefficient for relative air clearance, as shown in Table 2.1.

If we neglect the problems regarding three-dimensional flow and flow from stability trunks (internal skirts to divide the air cushion), then the air flow rate from the jet nozzles of the craft could be written as

$$Q = V_j t L_j \tag{2.3}$$

Table 2.1 Coefficient f relative to h/t

h/t	f
1	0.75
2	0.65
3	0.54
≥4	0.50

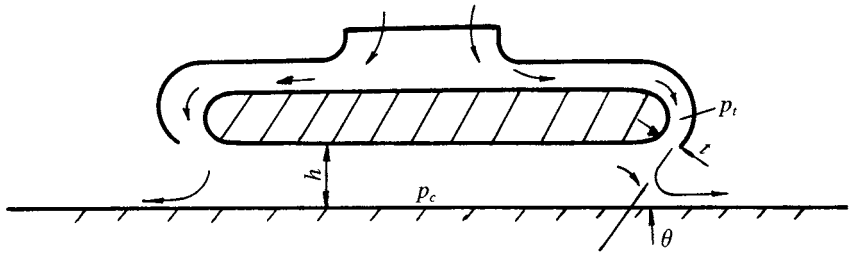

Fig. 2.1 ACV cushion cross-section.

where Q is the total flow rate jetted from the peripheral nozzle of the craft (m^3/s) and L_j the peripheral length of the nozzle (m). Then the lift power can be expressed by

$$N_{el} = QP_t/(75\eta_f\eta_d) \tag{2.4}$$

where N_{el} is the lift power of craft (kW), η_f the fan efficiency and η_d the air duct efficiency. Regarding the cushion pressure as uniformly distributed, then the weight of craft which can be lifted is

$$W = p_c S_c \tag{2.5}$$

where W is the weight of craft (N) and S_c the cushion area (m^2).

In order to develop a relation for N_{el} relative to W, we need to determine V_j. To do this we need to look at the various air jet theories.

Exponential theory for air cushion performance on a rigid surface

Thin nozzle theory was based on the assumption of infinite thinness, namely the jet velocity along the direction of nozzle thickness distributes uniformly. As a matter of fact, the jet velocity does not distribute uniformly because the back pressure of jet flow along this direction is rather different.

Mr Stanton-Jones of the British Hovercraft Corporation developed a relation based on the assumptions that the back pressure at the edge of nozzle, namely the side close to the atmosphere, was equal to the pressure of the atmosphere, and the back pressure at the inner edge of the nozzle was equal to p_c. The flow rate and total pressure of the lift fan can then be derived as

$$p_c/p_t = 1 - e^{-2x} \tag{2.6}$$

where

$$x = (1 + \cos\theta)t/h \quad \text{(as in equation 2.1)}$$

$$Q = [2/\rho_a].\ \{l_j h p_t^{0.5}\ [1 - (1 - p_c/p_t)^{0.5}]/(1 + \cos\theta)\} \tag{2.7}$$

These equations gave results which correlated with practical experience.

Theory for plenum chamber on a rigid surface [9]

Similar to thin peripheral jet theory, we assume that air flow is incompressible and non-viscous, but the flow streamline for the air escaping from the cushion periphery

is rather different from hovercraft with peripheral jets, because of its different duct configuration.

A typical transverse section for this type is shown in Fig. 2.2, similar to the craft '33' constructed by HSEI. The cushion flow is pumped from air ducts directly into the cushion rather than from peripheral nozzles as for a peripheral jet hovercraft.

Flow diffuses in the plenum chamber and forms the air cushion. For this reason, the relation may be derived simply because the pressure in the plenum chamber can be considered as a uniform distribution. In fact, this was validated by testing of manned craft, with the exception of hovercraft operating at high speed and with high-frequency heaving and pitching. Thus the unit flow rate around the craft periphery can be written as follows:

$$Q = \sqrt{[2p_c/\rho_a]}\, \Phi l_j \mu(j) h(j) \mathrm{d}j \tag{2.8}$$

where $\mu(j)$ is the discharge coefficient for the peripheral seals, in general 0.5–1.0, and $h(j)$ the air gap along the periphery of craft. Generally we take $\mu(j)$ and $h(j)$ as constants, so that the integration of the above expression can be written as

$$Q = [2p_c/\rho_a]\mu h l_j \tag{2.9}$$

The A. A. West single wall theory [10]

Flexible skirt configurations evolved from the peripheral jets, via the jetted bag skirt to bag and finger type skirts. Transverse sections showing these skirts are shown in Fig. 2.3.

The physical phenomenon with respect to bag–finger skirts now widely used in ACV/SES, is not suitable for explanation by the theories mentioned above, such as thin jet theory and exponential theory.

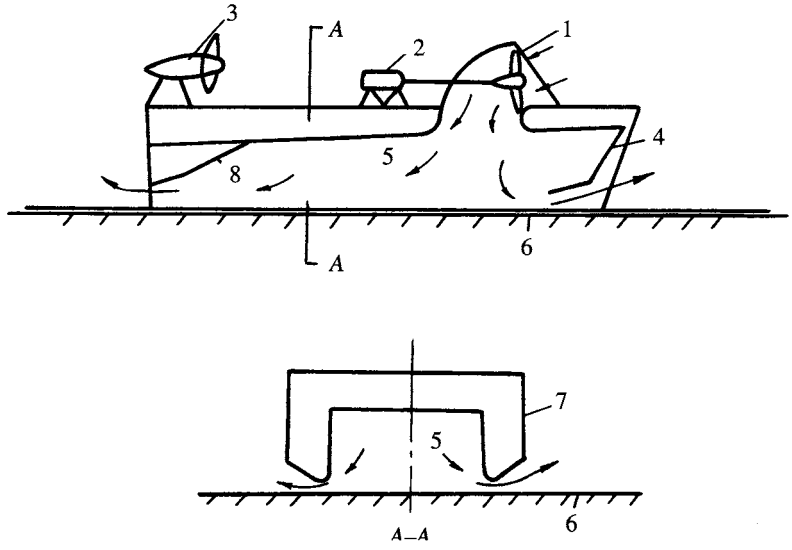

Fig. 2.2 Cross-section of SES with plenum chamber cushion. 1: lift fan, 2: lift engine, 3: propulsion engine and propeller, 4: bow seal, 5: air cushion plenum chamber, 6: rigid surface, 7: sidewall, 8: stern seal.

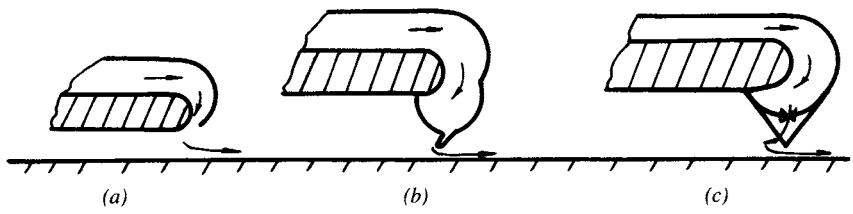

Fig. 2.3 Skirt configurations: (a) rigid peripheral jet; (b) inflated bag with short nozzles; (c) bag and finger type skirt.

A. A. West assumed that the flow completely stuck to the inner surface of the skirts as soon as it jetted from the nozzles in the bag, in the manner as shown in Fig. 2.4. He also assumed that:

- The total pressures along the section of jet were constant.
- At section e, part of the flow blows to the atmosphere and another part blows into the air cushion. Point B′ is its separation point.
- The static pressure along the nozzle (section j) is also constant.

Thus the flow momentum for the air jetted into the cushion, per unit length of nozzle, may be written as follows (cf. equations 2.1–2.4)

$$M_j = \rho_a V_j^2 t \tag{2.10}$$

According to the Bernoulli equation, the total pressure of the jet at the nozzle, the sum of the static pressure head and dynamic (kinematic) pressure, can be written as

$$p_t = p_c + 0.5\rho_a V_j^2$$

thus

$$M_j = 2(p_t - p_c)t \tag{2.11}$$

where V_j is the jet velocity at nozzle, t the nozzle thickness, p_c the cushion pressure and p_t the total pressure of the jet at the nozzle.

Meanwhile, it is assumed that the flow momentum per unit length of air curtain along the streamlines AA′ and BB′ to the atmosphere was M and remains constant at the locations e and o. On this basis there is no loss of flow momentum along the streamline AA′. This assumption was not precise, but it was proved realistic by the experimental results presented in the references of A. A. West's paper [10].

According to Newton's formula, the equation which describes the controlling section shown in Fig. 2.4 may be written as follows:

$$M_j \cos\theta + M_e = p_c h_b - p_0 h_s - \int_0^l p \sin\theta \, dl \tag{2.12}$$

where h_b is the vertical distance between the rigid bottom of the craft and the rigid surface, h_s the vertical distance between the lower tip of the single wall skirt and the rigid surface, p the static pressure of cushion air on the inner wall of the skirt, p_0 the atmospheric pressure, and l the length of the angled skirt wall.

The static pressure locally along the inner wall of a skirt is variable, hence the integral in the last term of equation (2.12). The closer it approaches the lower tip of the

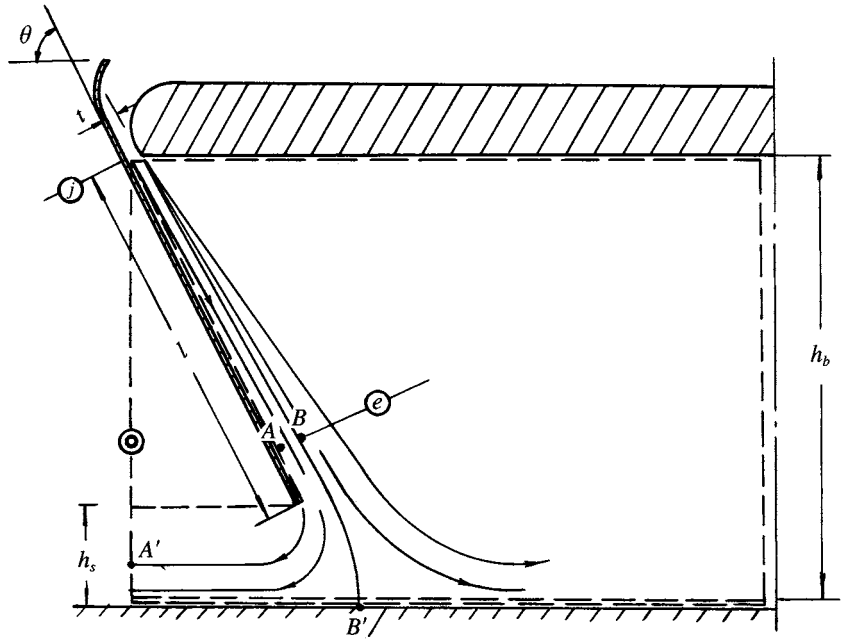

Fig. 2.4 Hypothesis for air jet streamlines based on A. A.West's single wall theory.

skirt, the lower the pressure and nearer to atmospheric pressure. However, globally it is reasonable to assume that the static pressure mentioned above is constant, namely cushion pressure p_c and then the above formula may be written as

$$M_j (\cos\theta + M_e/M_j) = (p_c - p_0)h_s \tag{2.13}$$

Based on the Mayer velocity distribution and boundary layer thickness for a two-dimensional jet with enclosing wall and turbulent flow, the ratio of flow momentum at section e to that at section j has been derived by A. A. West as follows:

$$M_e/M_j = 2.75\,(l/t)^{-0.45} = 2.75\,((h_b - h_s)/(t\sin\theta))^{-0.45} \tag{2.14}$$

where h_s is the air clearance of the nozzle.

Upon the substitution of equations (2.11) and (2.14) in equation (2.13), we have

$$\frac{p_c - p_0}{p_t - p_0} = \frac{1}{1 + \{h_s/[2t\cos\theta + 2.75\,((h_b - h_s)/(t\sin\theta))^{-0.45}]\}}$$

Thus, the flow rate per unit air curtain length can be written as

$$m = \rho_a[2(p_t - p_c)/\rho_a]^{0.5}\, t/h_s$$

or

$$\frac{m}{[\rho_a(p_c - p_0)]^{0.5}} = \left| \frac{1}{h_s[\cos\theta + 2.75\,((h_b - h_s)/t\sin\theta)^{-0.45}]} \right|^{0.5} \tag{2.15}$$

The lift power per unit air curtain area can be written as

$$N[\rho_a/(p_c - p_0)^3]^{0.5} = (2^{0.5}t/h_s)[1 + \{h_s/[2t\cos\theta + 2.75((h_b - h_s)/t\sin\theta)^{-0.45}]\}]^{0.5}$$

$$\times \{h_s/[2t\cos\theta + 2.75((h_b - h_s)/\mathrm{t}\sin\theta)^{-0.45}]\}^{0.5} \qquad (2.16)$$

where m is the flow rate per unit air curtain length and N the lift power per unit air curtain area.

While A. A. West's theory could be applied to real craft with a bag and finger skirt, the disadvantages of this approach would be as follows:

- The assumption made by West that the bag and finger type skirt may be simplified as a simple single wall skirt and the air curtain jetted from a nozzle stuck to the skirt finger does not agree with practice.
- The theory does not consider the effect of viscosity of air as a real fluid. Real flow conditions can be illustrated as in Fig. 2.5. Thanks to the viscosity of flow a lot of air will be ingested from the atmosphere into the air curtain to form a combined flow, namely the curtain jet flow m_c which will separate into two curtains, one to the atmosphere and another into the cushion.
- The theory does not consider the flow energy losses from nozzles in the bag. Clearly this is not reasonable for bag and finger skirts, though it is acceptable for open loop designs.
- It is not reasonable to assume zero energy loss between the flow streamlines AA′ and BB′, i.e. losses in a two-dimensional jet in a real fluid as against an infinitely thin jet.

2.3 Practical formulae for predicting air cushion performance

The various theories described above to predict the static air cushion performance of craft over ground, have disadvantages as follows :

- The theory based on a thin nozzle correlated with experimental results in the early research stage of hovercraft has precision at large hover heights (clear air gap), but is not realistic for small hovering heights, as is the case of craft with bag and finger skirts. This is because the air curtain jetted from under segments or fingers will be distorted by the proximity of the ground and the complex geometry of the finger itself.

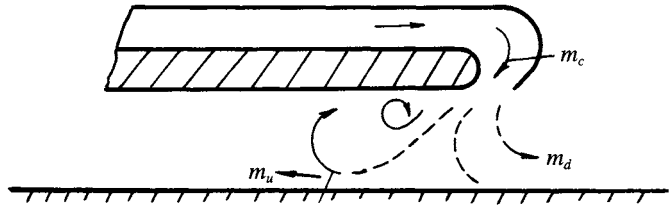

Fig. 2.5 Actual air streamlines including air viscosity.

- In order to simplify the formulae, the viscosity of air is not considered in the theory. This was because it was too difficult analytically to predict the air cushion characteristics including the viscosity (turbulence) of air flow. For air jet cushions, some approximations may be made, but for a segmented skirt, this becomes too complex for analytical treatment.
- The hydrodynamic performance of the bag and finger type flexible skirt will change dramatically from the above formulae, therefore some experts, such as Professor P. Kaplan [11], considered that the simple theory for craft with a plenum chamber is better applied to such skirts even though this approach is somewhat conservative.

The plenum chamber theory does not include the enclosing wall effect of the flow and for this reason experimentally derived methods for predicting static air cushion performance may be used to reduce the inherent conservatism. MARIC commenced the experimental investigation on static air cushion performance for two-dimensional flexible skirts on rigid surfaces in 1974. Since then the theories for three-dimensional skirts and also performance over a water surface have been investigated regarding the influence of the seal effect. This will now be outlined.

Experimental method and equipment

MARIC used two skirt test rigs as the main experimental method; a small rig (Fig. 2.6) was used for qualitative analysis and a larger one for quantitative analysis (Figs 2.7–2.9) to obtain a higher Reynolds number at its jet nozzles. The principal dimensions of the two rigs are listed in Table 2.2.

The full-scale skirt of a 50–80 t ACV can be simulated in the big test rig and the air flow rate can be measured by means of conversion from static pressure measurements

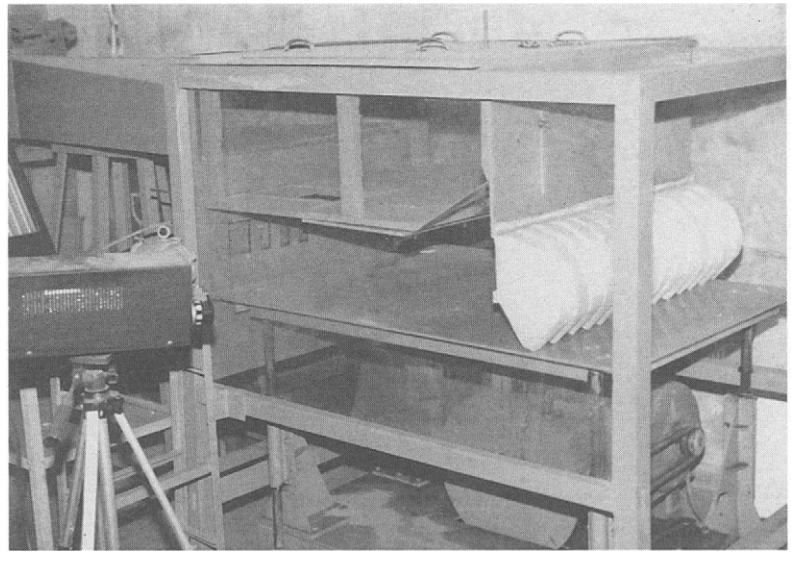

Fig. 2.6 MARIC's small skirt test rig.

Table 2.2 The principal dimensions for large and small sized MARIC skirt test rigs

	Small box	Big box
Box length (mm)	1050	4400
Box width (mm)	700	2230
Box height (mm)	1000	3350
Permitted max. height for test skirt (mm)	350	1500
Permitted max. width for test skirt (mm)	700	2200
Reynold's number, Re, for jet flow	$2 \times 10^3 \sim 4 \times 10^4$	$5 \times 10^4 \sim 2 \times 10^5$

at the air inlet of the centrifugal fan. In addition, air gap, cushion pressure and bag pressure can all be measured. The calculation error is small because of its relatively large size and the *Re* for flow in the jet can be above the minimum *Re* required for turbulent flow.

Test data obtained are more precise and stable from the large box. The box length is about 4 m, which was found to be the minimum length to give stable cushion pressure within the box (early experiments with skirt boxes had problems with unstable flow). This has been verified by experiments carried out.

We use the following main dimensional ratios of skirts for investigation (see Fig. 2.9):

$$H_1/H_2 \qquad S/B_b \qquad x/B \qquad \theta$$

where H_1 is the height of skirt bag, H_2 the height of fingers, S the area of the air feeding hole in each finger space, B_b the finger width, x the location of holes, relative to finger attachment and θ the angle of segment or finger outer face to the ground.

Tests for three sets of skirts were carried out in the small test rig, giving test sample data as shown in Table 2.3. It was found that influence of H_1/H_2 on static air cushion performance of a two-dimensional skirt was small. For this reason, for simplicity, we neglected the parameter H_1/H_2 to save on test time and expense on a large skirt box. Owing to the lower accuracy both for manufacture of the skirt and regulation of hovering height, as well as the irregular shape for small size of skirts, the errors for test

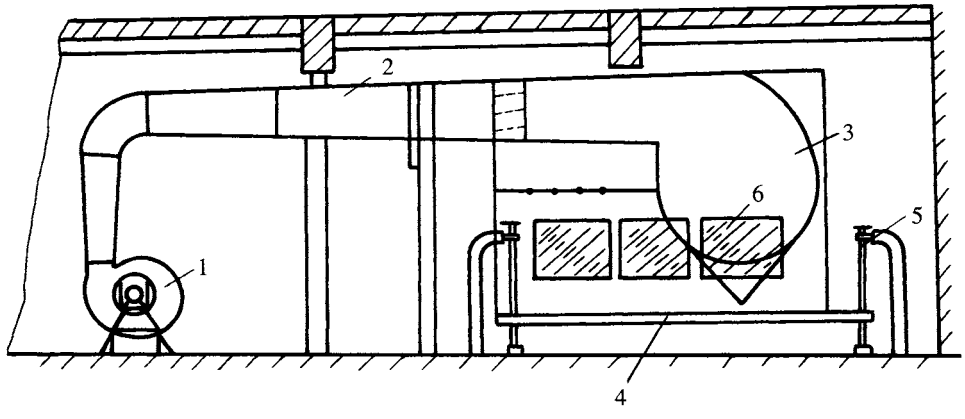

Fig. 2.7 Sketch of MARIC's large skirt test rig. 1: air supply fan, 2: air ducting system to skirt section, 3: skirt section, 4: movable ground plate, 5: ground plate oscillation system, 6: observation windows.

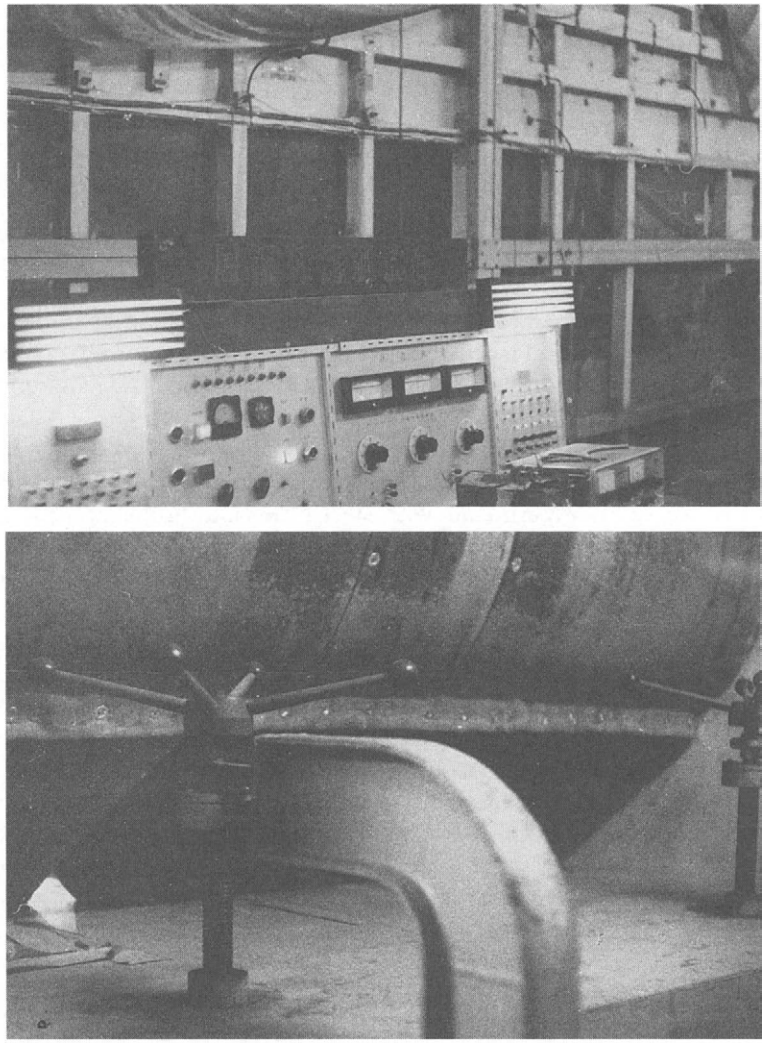

Fig. 2.8 Test section of the large skirt test rig: (a) side view; (b) skirt and movable bottom.

Table 2.3 Test sample data for small skirt test rig

$S/B_b = 0.0289$ $x/B = 0.512$	H_1/H_2
Project 1	0.715
Project 2	1.0
Project 3	1.285

results would be increased, thus the test data would be unstable and scattered. Nevertheless it could be used as a qualitative investigation for selecting the skirt configuration for test in the larger rig. The test sample data for the big skirt test rig are shown in Table 2.4.

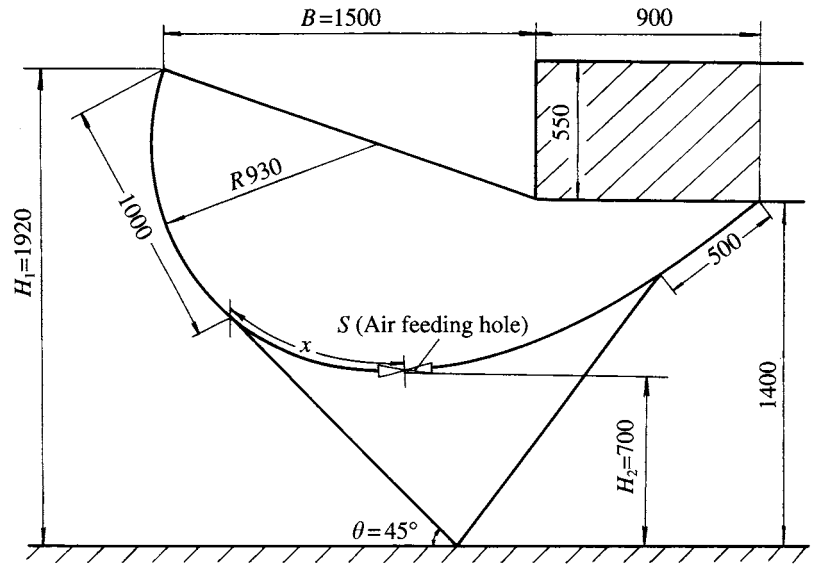

Fig. 2.9 Dimensions of typical bag and finger type skirt on the large skirt test rig.

Table 2.4 Test sample data for big skirt test rig

Items	x/B	S/B_b
1	0.512	0.0203
2	0.512	0.0289
3	0.512	0.0424
4	0.512	0.0610
5	0.512	0.0289
6	0.333	0.0289
7	0.700	0.0289

Analysis methods

The cushion pressure can be expressed by the following relations:

$$p_c = f\{h, H_1, H_2, b, t, v_j, Re_j, \ldots\} \tag{2.17}$$

where the geometrical parameters are as shown in Fig. 2.9 and h is the hover height, t the average nozzle thickness, $t = S/b$, v_j the jet velocity, Re_j the Reynold's number for the jet nozzle, $Re_j = v_j t/\upsilon$, and υ the kinematic viscosity coefficient. According to the theory of dimensionless analysis, this equation can be written as

$$\bar{p}_c = p_c/q_j = f_1\,(h/t, H_1/H_2, S/B_b, x/B, Re_j) \tag{2.18}$$

Bag pressure can also be written as follows:

$$\bar{p}_t = p_c/p_t = f_2\,(h/t, H_1/H_2, S/B_b, x/B, Re_j) \tag{2.19}$$

where p_t is the skirt bag pressure and $q_j = 0.5\rho_a v_j^2$.

Considering that the jet nozzle *Re* on the big skirt test rig is in the turbulent region and the effect of H_1/H_2 to p_c can be neglected, then the relative cushion pressure can be written as follows:

$$\bar{p}_c = f_1\,(h/t,\ S/B_b,\ x/B) \tag{2.20}$$

In order to save time for test and analysis and also considering that the foregoing formula should be processed by three-dimensional regression analysis, the test projects can be arranged as shown in Table 2.4 and also taking the $\bar{p}$ as the function of relative hovering height, namely $\bar{p}_c = f(h/t)$. Then the correction with respect to S/B_b and x/B can also be considered. The same method can be used with the other characteristics of hovercraft such as cushion flow rate coefficient, cushion power coefficient and skirt bag pressure coefficient to derive these as well. These coefficients can be written as follows:

$$\begin{aligned}
\bar{p}_c &= f_{pc}(h/t) \\
\bar{p}_t &= p_c/p_t &&= f_{pt}(h/t) \\
\bar{m} &= m/(\rho_a p_c)^{0.5} &&= f_m(h/t) \\
\bar{n} &= (N\rho_a^{0.5})/p_c^{1.5} &&= f_p(h/t)
\end{aligned} \tag{2.21}$$

where $\bar{p}_c$ is the cushion pressure coefficient, namely the relative cushion pressure, $\bar{p}_t$ the bag to cushion pressure ratio coefficient, $\bar{m}$ the cushion flow rate coefficient, $\bar{n}$ the cushion power consumption coefficient, $\bar{m}$ the mass flow rate per unit area of air curtain, $m = Q\rho_a/l_j h$, l_j the peripheral length (m), ρ_a the air density (Ns^2/m^4), Q the cushion volumetric flow rate (m^3/s) and N the power consumption of hovercraft per unit area of air curtain (Nm/s per m^2). All of the coefficients mentioned above are dimensionless.

Analysis of streamlines from tests

Due to the large size of the skirt test rig, the streamlines may be plotted (Figs 2.10 and 2.11) for two hovering conditions, one for large hovering height ($h/t < 1$) and one for small hovering height ($h/t \cong 0.15$).

The length and thickness of the enclosing wall for the jet (the total pressure of flow will drop dramatically outside such thickness so Pitot and total pressure measurements can be used to survey it), the total pressure and the separation point B can be measured. The streamline chart for large/small hovering height was obtained as shown in Figs 2.10 and 2.11 respectively. It is found that the following physical phenomena are observed:

- The length and effect of enclosure for a jet with definite angle can be found by testing, although in the case of the bag and finger skirt, in which the flow will diffuse suddenly at the location of holes, it will also be related to the location of the holes and hovering height.
- Owing to the effect of the enclosing wall on the jet, the air flow at the segment tip possesses the function of sealing the air cushion, especially in the case of large air clearance (Fig. 2.10) and the separation point *B* appears very close to the ground. Its position inside or outside the skirt tip line is dependent on the cushion pressure

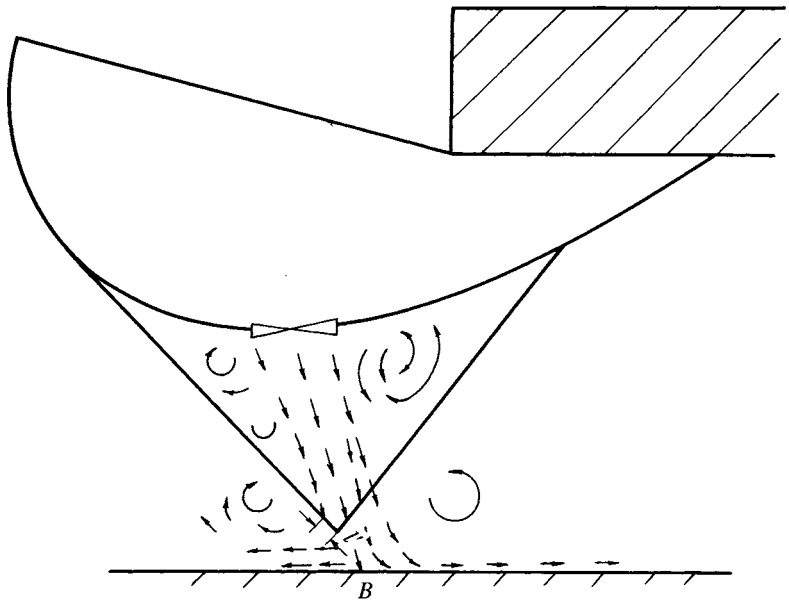

Fig. 2.10 Air streamline diagram at higher air clearance.

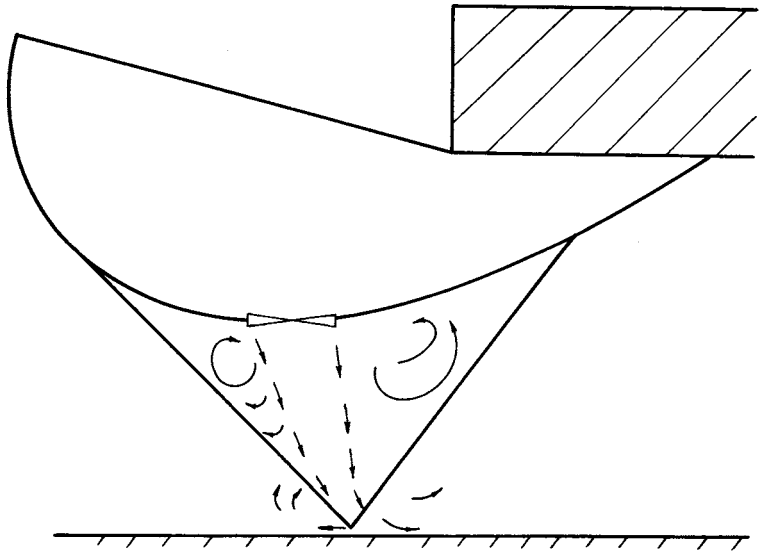

Fig. 2.11 Air streamline diagram at lower air clearance.

and the segment geometry. These factors can affect the dynamic response of the skirt in operation.

- A series of vortices is formed around the nozzle which causes some flow energy losses, but these do not affect cushion pressure very much because of its weak

vorticity, even though the range of vortices is rather large. Simultaneously, the test cushion pressure distributes uniformly.

- According to analysis of the streamline charts, it is found that the location of the feed holes in the bag will affect the jet flow enclosing length and consequently the air cushion performance.

  For this reason, an optimum hole location x/B and relative area of hole S/B_b may be found. The best location is generally close to the segment upper attachment, though some experimentation is necessary for optimization, once the overall skirt section has been designed. This is always a worthwhile exercise.
- Owing to the enclosing effect of the jet flow assisting sealing of the air cushion, this is equivalent to a reduced flow coefficient during leakage of air from a small hole to the atmosphere, consequently the approach will be to concentrate on defining the relative flow coefficient $\bar{m}$ and cushion pressure coefficient $\bar{p}_c$ at different ground clearances (air gap under skirt tip).

Experimental results and analysis

The loss of air (leakage) between the skirt and box wall has to be considered, which leads to the equivalent air clearance of the skirt h, and can be written as

$$h = h_0 + h'$$

where h_0 is the actual air clearance of the skirt, namely, the vertical distance between the lower edge of the skirt finger and the ground, and h' the equivalent air clearance of skirt considering the air leakage loss between the skirt and box wall as well as the gap between the fingers. The air leakage therefore has to be corrected in the case of fitting a regression line for cushion flow derived from the test results. The following observations were made at MARIC:

1. It was found that the test results are concentrated, having a small standard deviation, which was also verified by test results gathered for another series which was carried out one year later. The test data were considered stable and the selected parameters to be reasonable.
2. For a conventional bag and finger type skirt, with parameters such as $H_1/H_2 = 1$; $x/B = 0.512$; $S/B_b = 0.0289$; the cushion pressure coefficient $\bar{p}_c$, cushion flow rate coefficient $\bar{m}$, bag and cushion pressure ratio $\bar{p}_t$ and cushion lift power coefficient $\bar{N}$ can be regressed to the following expressions (see Figs 2.12, 1.14 and 1.26):

$$\bar{p}_c = p_c/q_j = 0.602\,(h/t)^{-0.403} \tag{2.22}$$

$$\bar{p}_t = p_c/p_t = 0.638\,(h/t)^{-0.49} \tag{2.23}$$

while

$$h/t < 1.05 \quad \bar{m} = m/(\rho_a p_c)^{0.5} = 0.625\,(h/t) - 0.415 \tag{2.24a}$$

$$h/t > 1.05 \quad \bar{m} = m/(\rho_a p_c)^{0.5} = 0.848 - 0.147\,(h/t) \tag{2.24b}$$

$$h/t = 1.05 \quad \bar{m} = m/(\rho_a p_c)^{0.5} = \text{average of (equations 2.24a and b)}$$

These expressions are suitable for h/t between 0.4 and 2.5; alternatively, the following may be used:

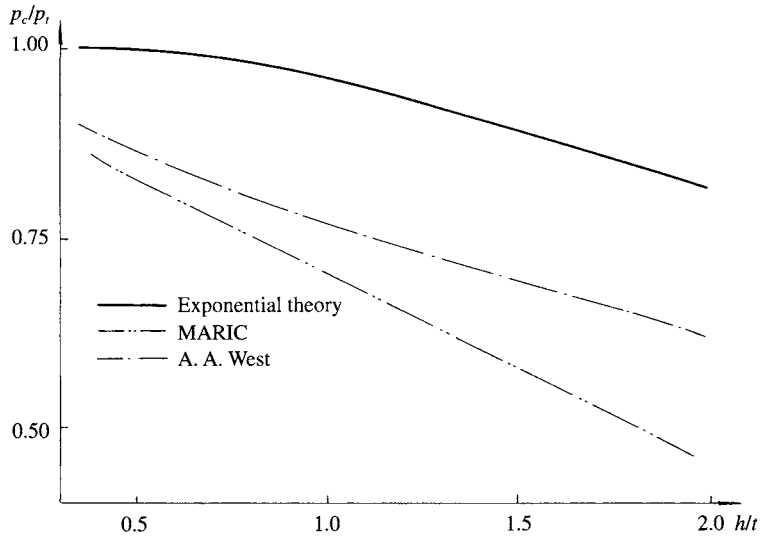

Fig. 2.12 Comparison of bag / cushion pressure ratio versus h/t between various theories.

$$\bar{m} = \mathrm{m}/(\rho_a p_c)^{0.5} = 0.632\,(h/t)^{-0.336} \tag{2.25}$$

$$\bar{N} = (N\rho_a^{0.5})/p_c^{1.5} = 1.05\,(h/t)^{-0.067} \tag{2.26}$$

This equation can be corrected with regard to various x/B and S/B_b, as described in [12].

3. The optimum location of x/B can be derived as $(x/B)_{opt} = 0.48$–0.54. It seems that this is not in relation to h/t, i.e. the air curtain can be sealed as long as the flow jetted from the nozzle can attach to the skirt wall, even though only a little way up the segment. The effect will reduce in the case of $x/B > 0.54$ and the effect of the jet enclosing wall will be enhanced in the case of small x/B, but at a penalty of increasing internal flow losses.
4. The loss across the nozzle jet increases as the area of the nozzle decreases, i.e. p decreases inversely with p_t.
5. The calculated results from exponential theory, the theory of A. A. West, plenum theory and MARIC theory may be compared and discharge coefficient μ applied to plenum chamber theory. The results can be written as [9]

$$\mu \approx 0.5 + 0.05\,(\pi/2 - \theta')^2$$

or

$$\mu = 0.5 + 0.4 \times 10^{-3}\,\theta' + 0.109 \times 10^{-4}\,\theta'^2 - 0.494 \times 10^{-7}\,\theta'^3 + 0.345 \times 10^{-9}\,\theta'^4$$

where θ' is the inclination angle of the skirt finger. We take $\mu \cong 0.53$ where $\theta = 45°$

It is found that the value of $\bar{m}$ from test results is smaller than that given by the formula from plenum chamber theory, in the case of $h/t > 0.6$, because the jet flow

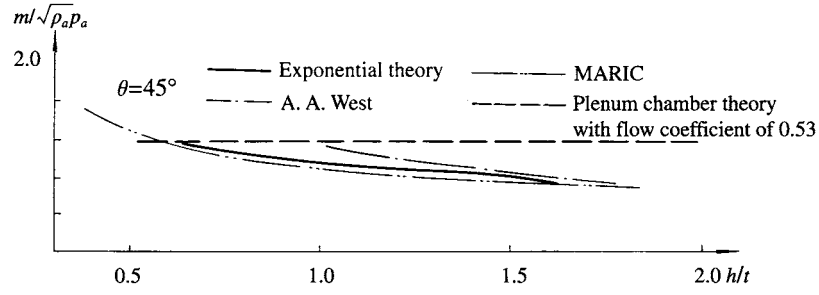

Fig. 2.13 Comparison of air flow coefficient between various theories: exponential theory; A. A. West theory; MARIC theory; plenum chamber theory with air flow rate coefficient of 0.53.

follows the angle of the wall of the finger, consequently contracting the cushion outflow jet so as to reduce the cushion flow rate.

From the figure the greatest difference in $\bar{p}_t$ is found between the test results and the results calculated by the exponential formula and the West formula in the case of large h/t values. However, all of them will be closer in the case of smaller h/t. The test result for the cushion lift coefficient (Fig. 2.14) is higher than that calculated from the exponential and A. A. West's theories, because the experiments accurately simulate the losses through the feed holes of bag–finger skirts and the weak effects of the jet enclosing the walls.

6. The effect of the skirt material on the static air cushion performance. Reference 13 listed eight test samples with different materials which are shown in Table 2.5. The test results showed the effect of specific weight of skirt material on the static shape of skirts.

   It is found that skirt material characteristics do not greatly affect the static air cushion performance in the case of any given configuration and hovering height of the skirts. The effect of skirt material characteristics on the hovering height can therefore normally be neglected and the hovering height can be measured directly during tests. The effect of specific weight of skirts on the geometric shape will be described in Chapter 7. From such tests it is also found that the effect of elasticity of skirt material on the shape of the skirt is weak.

Table 2.5 Experimental samples of skirt for various skirt materials [14]

Model	Scale ratio λ	Width of air duct/ width of bag	Equivalent nozzle width/0.095	Skirt material	Test equipment
1	1	0.625	1	9514 Rubber core	Large rig
2	1	1	1	9514 Rubber core	Large rig
3	1/2	1	1	6408 Rubber core	Large rig
4	1/2	1	1/2	6408 Rubber core	Large rig
5	1/2	1	1/2	1533 Rubber single surface coating	Large rig
6	1/2	1	1	1533 Rubber single surface coating	Large rig
7	1/8.9	1	1/8.9	Plastic diaphragm	Small rig
8	1/8.9	1	1/8.9	9514 Rubber core	Small rig

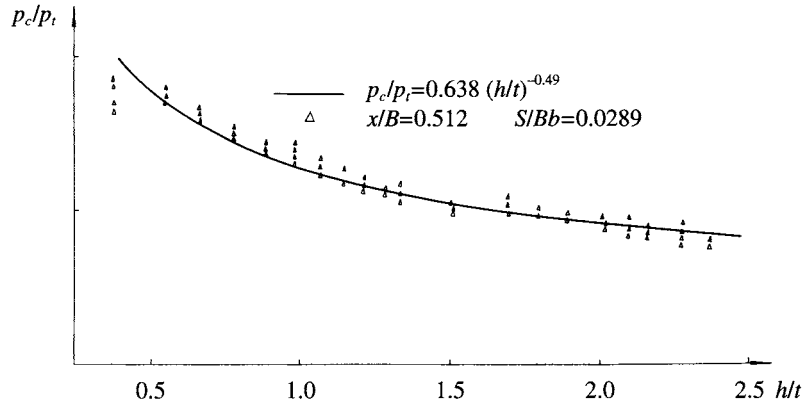

Fig. 2.14 Relation between bag/cushion pressure ratio p_c/p_t and relative air gap h/t.

7. Scale effect. From the tests described above, it was found that the Re_j greatly affects static hovering performance of skirts. In general the turbulent flow region can be established as $Re_j > 8 \times 10^4$.

   In the experiments themselves the data points do not scatter, as long as $Re > 10^5$. Because the Re on the small skirt test box is smaller than that on the large box, in general $Re_j = 1.1\text{–}2.4 \times 10^4$ for the small box, this leads to greater scatter and to errors in evaluated $\bar{p}_c$, $\bar{m}$ and $\bar{p}_t$. It demonstrates that the air clearance of model craft is less than that of full-scale craft even though the fans, air ducts and the geometric configurations for both are similar, because the model Re is less than the critical Re, i.e. $< 10^5$.

   For this reason, model simulation experimental results gain an error not only from static hovering tests in a skirt test box, but also calm water resistance tests and seaworthiness tests because of their low Re and thus lower air clearance of models. Sometimes, in order to eliminate such errors, one increases the revolution of model fans deliberately, to increase the air gap, since one would rather be similar on air clearance than the dynamic simulation on model fans.

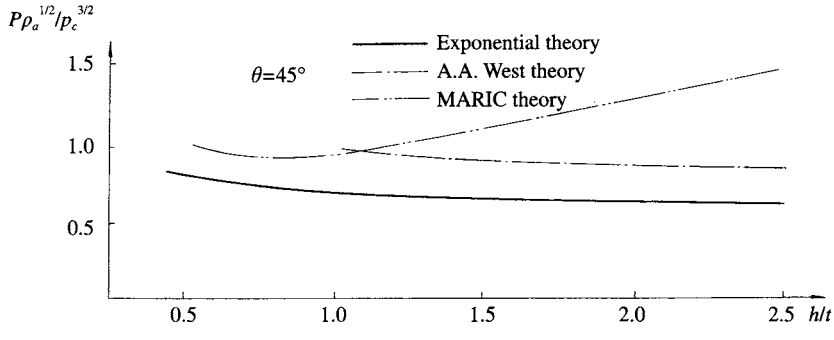

Fig. 2.15 Comparison of lift power output coefficient between various static air cushion theories.

2.4 Static air cushion characteristics on a water surface

Static hovering performance of SES on water

The various shapes of mid-sections of sidewalls are shown in Fig. 2.16; a typical one is figure (a), namely sidewalls with perpendicular inner and outer walls near the water surface. The craft total weight is supported by a combination of cushion lift and buoyancy of the sidewall, which can be expressed as

$$W = p_c S_c + 2V_0\gamma_w \tag{2.27}$$

where W is the craft weight (N), p_c the cushion pressure (N/m^2), S_c the cushion area (m^2), V_0 the volumetric displacement provided by each sidewall (m^3) and γ_w the specific weight of water (N/m^3).

According to Archimedes' principle, the relationship between cushion beam, inner and outer drafts and width of sidewalls with different shape can be determined by the following expressions and those in Fig. 2.16:

$$S_c = B_c l_c \tag{2.28}$$

$$t_o - t_i = p_c/\gamma_w \tag{2.29}$$

where t_o is the outer draft of sidewalls (m), t_i the inner draft of sidewalls (m), l_c the cushion length (m), B_c the cushion beam (m) and w the calculating width of sidewalls (m). The inner sidewall draft gradually reduces as lift power is increased and cushion air will leak from under both sidewalls once the cushion pressure exceeds the inner sidewall draft (Fig. 2.17), as well as under the bow and stern seals, and form the plenum type of craft, similar to the craft model '33' of HSEI and the US Navy SES–100B. The drag of this type of craft decreases dramatically as lift power is increased.

The outer draft of sidewalls, t_o, is dependent upon the lift fan(s) flow rate and the inner draft, t_i, is dependent upon the cushion pressure p_c. The air leakage from the

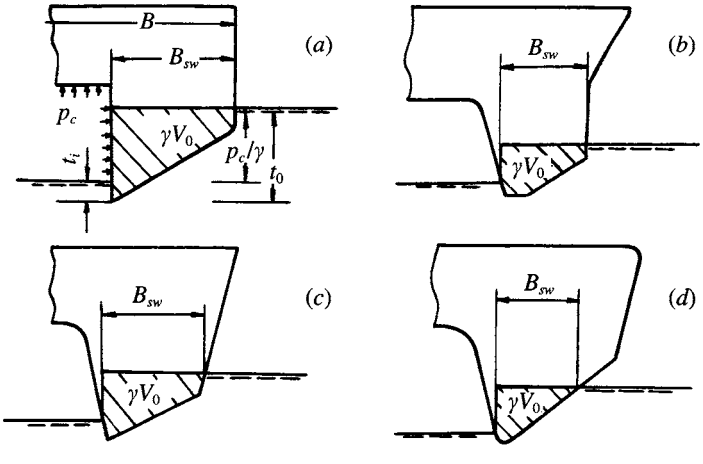

Fig. 2.16 Sidewall thickness on various sidewall configurations.

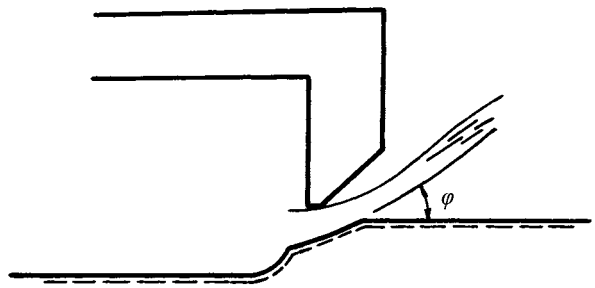

Fig. 2.17 Air leakage under SES sidewall with large air flow rate, hovering static over water.

cushion at the bow (also at the stern), can be illustrated as in Fig. 2.18. The flow rate of an SES hovering statically on a water surface is normally calculated using the following assumptions:

- The air flow is non-viscous and incompressible.
- For simplicity, the outlet flow streamline chart can be considered as Fig. 2.18 and takes the actual air clearance as $\phi(z_b - t_i)$ because of considering the contraction of leaking air flow, where z_b is expressed as the bow seal clearance, namely the vertical distance between the craft baseline and the bow seal lower tip. ϕ is the flow contraction coefficient at the bow seal.
- The distribution of static pressure for leaking air flow is a linear function. As shown in Fig. 2.18, the static pressure of leaking air flow is $p_\eta = p_c$ for $\eta = 0$, but while $\eta = (z_b - t_i)\,\phi$, $p_\eta = 0$, where represents the ordinate with the original point B and upward positive.

Thus the static pressure of leaking air flow at any point can be represented by

$$p_\eta = p_c[1 - \eta/(\phi(z_b - t_i))] \tag{2.30}$$

According to the Bernoulli theory, the horizontal flow velocity at any point between AB can be represented by following expression:

$$0.5\rho_a U_\eta^2 = p_c - p_c[1 - \eta/(\phi(z_b - t_i))\,] = p_c\eta/(\phi(z_b - t_i)) \tag{2.31}$$

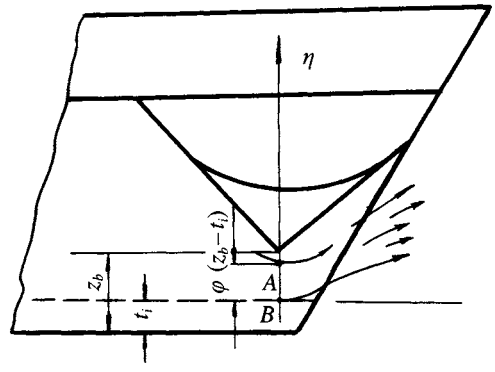

Fig. 2.18 Air leakage under SES bow seal hovering static over water.

where $U\eta$ is the leaking air flow speed in the horizontal direction. It is clear that the flow rate leaking under the bow skirt can be represented by

$$U_\eta = (2p_c\eta)/(\rho_a\phi(z_b - t_i))$$

then

$$Q_b = B_c\int_0^{\varphi(z_b - t_i)} U_\eta d\eta = 2/3\, B_c\phi(z_b - t_i)[2p_c/\rho_a]^{0.5} \tag{2.32}$$

As a consequence, the air cushion flow for craft statically hovering on a water surface is equal to 2/3 of that on a rigid surface, because of the action of back pressure of leaking air.

This estimate is approximate, but realistic and is generally applied as a method of estimation of the flow rate of an SES, because of its simplicity and the difficulty in measuring the steady flow in an SES on a water surface. By the same logic, the flow leaking from the stern seal can be obtained by this method; consequently, the total flow for craft hovering statically on the water surface can be obtained.

It is useful to note that the same reduction in air leakage rate also applies to an ACV hovering over water rather than land.

The static air cushion performance of ACVs on a water surface

The difference between the ACV and SES for static air cushion performance is that the sidewalls provide buoyancy. The typical static hovering attitude of an amphibious ACV can be seen in Fig. 2.19. If one neglects the reaction of the perpendicular components of jets flowing from peripheral and stability nozzles (the value of which is small in the case of small skirt clearance with a bag–finger type), then the cushion lift can be written as

$$\left.\begin{aligned} W &= p_c S_c \\ S_c &= l_c B_c \end{aligned}\right\} \tag{2.33}$$

where l_c and B_c are the cushion length and beam, which can be measured from the line on the plan of the water surface, which the lower tip of skirt is projecting on.

From Fig. 2.19, it is found that the craft weight is equal to the weight of water displaced from the depression; for this reason, the actual skirt clearance is equal to the

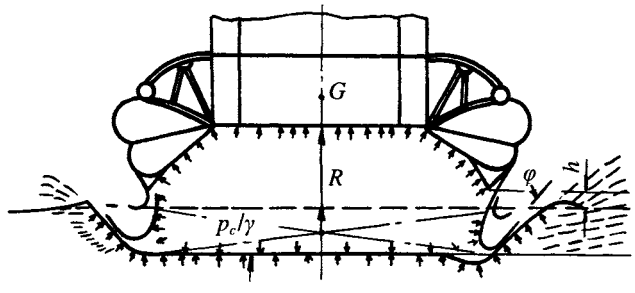

Fig. 2.19 ACV hovering static on water.

vertical distance between the lower tip of the skirt and an undisturbed water surface. Owing to the application of bag and finger skirts and the improvement in performance through development, skirt clearance on a water surface has decreased year by year.

One can observe that the skirt clearance on a water surface is very small on modern ACVs and sometimes the value may be negative for larger craft with responsive skirts. Therefore, it is suggested that cushion air flow can be calculated by plenum chamber theory or the foregoing methods applied to SESs. The peripheral jet requires much higher air flow to seal the air cushion in the case where the craft hovers with a significant gap to the calm water surface.

It is noted that the hovering process for an ACV with flexible skirt is more complicated, and is shown in Fig. 2.20, in which the numbers are explained as follows:

1. This represents that the craft floats off cushion statically on a water surface, the draft of craft is T_0.
2. Lift fan starts to operate, but owing to the low revolutions, fan pressure is low, therefore $T < T_0$. Though the craft is partially supported by air pressure, the draft of the buoyancy tank is still larger than zero to provide partial support of the craft.
3. Fans speed is continuously increasing. In the case of $T = 0$, namely zero draft of the buoyancy tank, then the weight of the craft will be completely supported by cushion lift.
4. The fan speed is increasing further, pressure remains almost constant while flow rate is increased, thus the skirts begin to inflate. A positive hull clearance h' begins to be gained, but smaller than design hull clearance.
5. The hull clearance is equal to design value h_s', a large amount of cushion air is now leaking under the peripheral skirt, the volume being dependent on the fan characteristic and lift power.

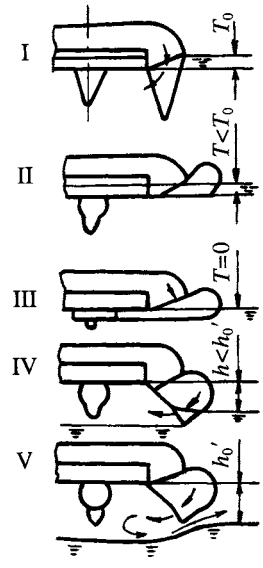

Fig. 2.20 Various static hovering positions of an ACV.

The air cushion characteristic curves for both ACV/SES are shown by Fig. 2.21 (the calculation in detail can be found in Chapter 11, Lift system design), where

- H_j–Q represents the characteristic curve of lift fans, p_t–Q represents the characteristic of the air ducting, i.e. the characteristic curve of a fan at any given revolution minus the pressure loss of flow in air duct, p_t represents the bag pressure of skirts and p_t–Q also represents the characteristic of the bag.
- p–Q represents the characteristic for static air cushion performance, namely the relation between flow and bag pressure at various hovering heights, which can be obtained by the foregoing formula. For this reason, the curve p–Q represents the relation between the bag pressure and flow rate and p_t–Q denotes the total pressure of air duct (or bag) at various hovering heights and fan revolutions.

The intersection point of both curves represents the hovering height of the craft at a given craft weight (a given cushion pressure) and any given fan speed. Hence, the air cushion characteristic curve for an ACV can be described as follows (also similar for an SES):

1. The minimum fan speed for inflating the skirt of an ACV (similar to the hovering attitude 4 in Fig. 2.20), will be that at which the total pressure of the lift fan equals the cushion pressure at the zero flow rate. At this point the craft weight is supported by cushion lift perfectly, but without having risen from the static condition. In the case of zero flow rate the total pressure of the fan is equal to the total pressure of the duct bag and thus to the cushion pressure.
2. The factors necessary for hovering the craft, i.e. from attitude 1 transient to attitude 3, is that the bottom of the buoyancy tank has to leave the water surface in order to exert the cushion pressure to the bottom and lift the craft. At MARIC

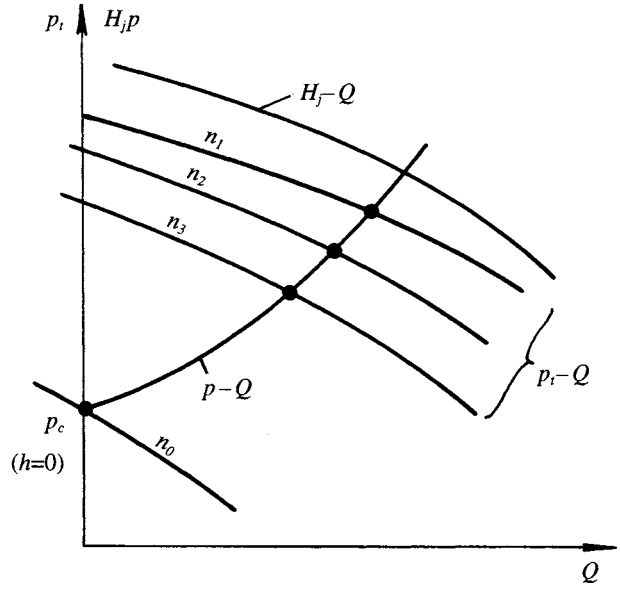

Fig. 2.21 Air duct and air cushion characteristics curves of ACV/SES.

there is experience that a hole for take-off has had to be installed in the craft bottom or skirt near the water surface (Fig. 2.22) in order to blow off the water in the cushion in order to exert cushion pressure on the bottom, because the height of a skirt of a jetted bag type (say, $H > 1$ m for medium-sized ACV) is always higher than the cushion pressure measured by the water head (namely $p_c < 0.3$ m H_2O).

3. The minimum fan speed of an SES for static hovering can also be defined, namely the condition of zero flow is equivalent to the situation that the inner draft of sidewalls t, has to equal the bow/stern clearance and also satisfy the following equation:

$$W = P_{c0}S_c + V_{i0}\gamma$$

where P_{c0} is the cushion pressure, namely, the fan total pressure at given speed and zero air flow rate, S_c the cushion area, at the sidewall draft for zero flow from bow and stern seals, V_{i0} the displacement (volumetric) of the sidewalls at W the weight of craft. This is the same draft, the necessary condition for an SES hovering in such a mode, namely the cushion air just blows off under the bow/stern skirt (not under the sidewalls).

It should be noted here that it is important for sidewall craft to have a positive value of t_i (Fig. 2.16) so that air is not leaked under the sidewalls. Experience suggests that t_i should be 15–20% of t_o. Below 15% air will start to be lost under the keels in relatively small sea states, restricting performance. SES may also need deeper draft and t_i at the stern to prevent propeller cavitation or water jet ingestion of cushion air. Sometimes a fence, or keel extension may be installed to help solve this problem.

2.5 Flow rate coefficient method

The relation between the cushion air flow rate and pressure for craft hovering on a rigid surface and calm water has been derived. However, the bag and finger type skirt with a small number of large holes for feeding the air into the air cushion from the

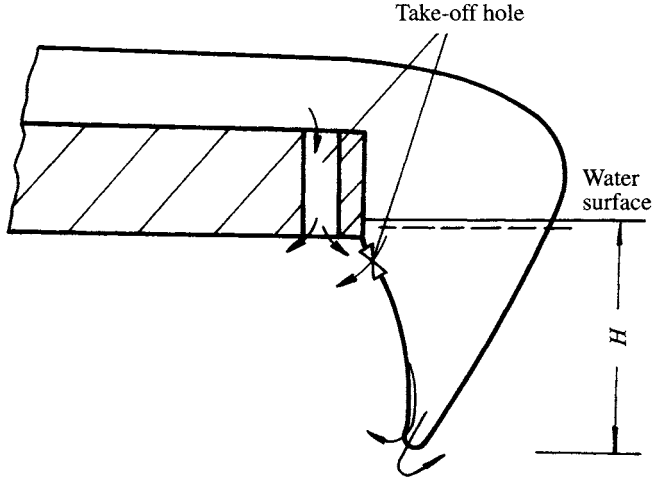

Fig. 2.22 Take-off holes on an ACV.

higher pressure bag is improved by the arrangement of a larger number of small feeding holes. This design improves the strength of skirt bags by reducing stress concentrations and thus the tendency to tear after fatigue due to operation.

The air cushion characteristics of such skirts are closer to those represented by plenum chamber theory. Moreover, the take-off performance and obstacle clearance ability is improved, therefore the flow for the take-off to the planing condition over water is not such an important parameter as concerned designers in the early stage of ACV/SES development. For this reason, rather than spend time on deriving the mathematical expressions for predicting the static air cushion performance, we take the flow rate coefficient $\bar{Q}$ as the factor to represent the static air cushion performance of craft. The relation for $\bar{Q}$ can be written as

$$Q = \bar{Q} S_c \sqrt{(2p_c/\rho_a)} \tag{2.34}$$

In general, we take the values of $\bar{Q}$ to be [15] :

$$\bar{Q} = 0.015 - 0.050 \quad \text{for ACV}$$

$$\bar{Q} = 0.005 - 0.010 \quad \text{for SES}$$

The required value of $\bar{Q}$ is related to the following performance factors:

1. craft drag at full or cruising speed on calm water;
2. take-off ability;
3. seaworthiness;
4. longitudinal/transverse stability of craft;
5. resistance to plough-in, etc.

Acceptable craft performance can normally be obtained if the cushion air system is designed with $\bar{Q}$ in the range above. The quoted range is rather large when designing a large SES or ACV and so it is normally best to start with the lower value (suitable for calm water operation, medium-speed craft) and then assess the additional flow required for items 2 to 5. These factors will be discussed further in following chapters.

As an alternative, particularly for amphibious ACVs, one often takes the skirt clearance of the craft hovering on a rigid surface as the factor to characterize its hovering ability and so to design the lift system. This is a common approach of designers because it is easy to measure the skirt clearance of an ACV both in model and full-scale craft. Although it is not accurate for the reasons outlined in the discussion of the various air jet theories above, it is easier to compare with other craft (or models).

Typically, for smaller amphibious craft the following relation is used:

$$Q = V_c D_c h L (\text{m}^3/\text{s})$$

where

$V_c = \sqrt{(2p_c/\rho_a)}$, the cushion air escape velocity (m/s),

$\rho_a = 1.2257 \text{ kg/m}^3/9.8062 = 0.12499 \text{ (kg m/s}^2\text{)}$

$= (0.07656 \text{ lb/ft}^3/32.17 = 0.00238 \text{ slug/ft}^3 \text{ in imperial units})$

D_c = nozzle discharge coefficient (2.3.4 item 5), $D_c \cong 0.53$ for 45° segment, L = peripheral length of cushion at the ground line (m) and h = effective gap height, typically $0.125 \times$ segment width, or if it may be assumed that segment width is approximately $h_c/2.5$ then $h = 0.05\, h_c$. Thus

$$Q \cong 2.12hL\sqrt{p_c} \tag{2.34a}$$

This relates the required flow to the escape area and should result in a small free air gap under the inflated segment tips of a loop and segment skirted craft over concrete.

2.6 The 'wave pumping' concept

The flow rate, calculated by equation (2.34), may only meet the requirements of skirt clearance for a craft hovering on calm water. As a matter of fact, craft often operate in rough seas, in which the craft pitches and heaves. Therefore designers have to calculate the vertical motion of craft in waves so as to determine the average required flow; this will be demonstrated in detail in Chapter 8.

Here we introduce a concept [16], namely wave pumping, which deals with the extreme hovering attitude of craft in waves. We assume that the cushion inflow rate of craft operating in waves will stay constant, namely the same as that in the static hovering condition. Thus the cushion flow changes as the volume occupied by the wave which is passing through the craft changes, as shown in Fig. 2.23.

Consequent to this, the cushion pressure will fluctuate because of the fluctuation of cushion outflow while constant inflow rate and the incompressibility of cushion air are assumed. Thus, the motion caused by fluctuating cushion pressure is called 'wave pumping' motion. To simplify the calculation, we assume as follows:

- Cushion air is incompressible.
- Waves are simple sinusoidal waves.
- Skirt clearances at bow/stern seals are constant, while the craft operates in head waves.
- The wave peak will never contact the wet deck of craft.
- The lowest edge of the cushion (i.e. the base line of sidewalls) coincides with the horizontal line of trough, namely no air leakage under the sidewalls.

Two typical situations for wave pumping motion of craft operating in waves are shown in Table 2.6. In fact we may assume that the SES can operate in one of three following modes.

First operation mode – platforming

In this mode of operation, the ACV or SES cannot respond to the waves, normally short steep chop, and so as wave peaks pass through cushion pressure is raised, and

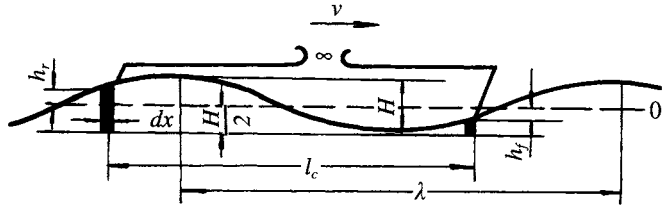

Fig. 2.23 Platforming of SES in waves.

Table 2.6 Craft operational modes with respect to the wave pumping motion

Operation mode due to wave pumping	Running attitude	Cushion over wave crest	Cushion over wave trough
Mode 1	Platforming	Air blown off from cushion	Air feed to cushion to fill cavity
Mode 2	Cushion volume constant	Craft lifted up	Craft drops down

as a trough passes, the air gap under the skirts increases and volume flow increases. The result is a rapid oscillation in the fan characteristic and vibration felt by operators. If lift power is not increased, skirt drag increases and speed reduces, often with a bow-down trim induced and in very short chop possibly a plough-in tendency. In very small sea states, small vibrations can be induced, which feel rather like driving a car over cobbles, hence the effect is called 'cobblestoning'. Normally this only occurs in craft which have a cushion with high volume flow rate.

Second operation mode – constant cushion volume

If the flow rate and cushion volume are held constant, keeping the lift power output at a minimum, then a definite vertical acceleration will exert on the craft because of wave pumping motion. Thus the maximum vertical acceleration can be derived under the action of pumping as follows:

$$(d_z^2/d_t^2)_{max} = [\pi v^2]/[\,10 \times l_c\,] \tag{2.35}$$

This calculation is approximate, because a lot of assumptions have been made. In particular, the heave and pitch motion of the craft in waves and air leakage around the sides of cushion have not been considered, therefore the calculation is very simple and does not demonstrate the seaworthiness quality of the craft.

It does, however, indicate the acceleration which will occur if the craft follows the wave surface profile, where no reserve lift power or inflow rate is available. To reduce this, it is necessary to allow the skirt to respond to the waves, which will then allow air to be pumped out of the cushion. An example calculation for this is given below. The aim of this calculation is to help designers to consider the reserve of lift power which is needed to be available to counteract the extreme motion of craft operating in rough seas.

Third operation mode – combination of first and second modes

The cushion pressure, cushion volume and the height of wet deck relative to the water surface are changed together, namely trading-off both the foregoing motions. In practice this is the mode which practical ACVs operate in.

Platforming analysis

The first mode is platforming, i.e. the cushion pressure and the vertical position of the wet deck remain constant, then the vertical acceleration will also be constant. This is the ideal operating attitude of craft and what the designer requires. However, one has

to regulate the lift power and lift inflow rate to keep the cushion pressure constant. This condition is also the one which will absorb the greatest volume of air; therefore we will make an analysis of this case.

When the craft moves along the x-axis for a distance of dx, then the change of water volume in the cushion can be expressed by the change of water volume at the bow/stern of the craft as shown in Fig. 2.23, then

$$dV = B_c[(H/2 + h_f)dx - (H/2 + h_r)dx] \tag{2.36}$$

where H is the wave height, h_f the bow heave amplitude relative to the centre line of the waves, h_r the stern heave amplitude relative to the centre line of the waves and B_c the cushion beam. Thus

$$\frac{dV}{dt} = b_c[(H/2 + h_f) - (H/2 + h_r)]\frac{dx}{dt}$$

because $dx/dt = 0$,

$$dV/dt = B_c\,(h_f - h_r)\,v$$

where v is the craft velocity relative to the waves.

The wave profile can be expressed by

$$h = (H/2)\sin a$$

where $a = 2\pi x/\lambda$, thus

$$a_f = a_r + 2\pi l_c/\lambda$$

where h is the wave amplitude, l_c the cushion length and λ the wave length. Therefore

$$\frac{dV}{dt} = \frac{B_c H}{2}(\sin a_f - \sin a_r)\,v$$

$$= \frac{B_c H}{2}\left[\sin\left(a_r + \frac{2\pi l_c}{\lambda}\right) - \sin a_r\right]v$$

$$= \frac{B_c H v}{2}\left[\left(\cos\frac{2\pi l_c}{\lambda} - 1\right)\sin a_r - \sin\frac{2\pi l_c}{\lambda}\cos a_r\right] \tag{2.37}$$

In order to determine the maximum instantaneous wave pumping rate, we take the first derivative of function dV/dt with respect to a equal to zero, then

$$\frac{d}{da}\frac{dV}{dt} = \frac{B_c H v}{2}\left[\left(\cos\frac{2\pi l_c}{\lambda} - 1\right)\cos a_r - \sin\frac{2\pi l_c}{\lambda}\sin a_r\right] = 0$$

This expression can be written as

$$\tan a_r = (\cos(2\pi l_c/\lambda) - 1)/\sin(2\pi l_c/\lambda) \tag{2.38}$$

Substituting expression (2.38) into (2.37), the maximum instantaneous wave pumping rate can be written as

$$\left(\frac{dV}{dt}\right)_{max} = \frac{B_c H v}{2}\left[\left(\cos\frac{2\pi l_c}{\lambda} - 1\right)\sin a_r - \left[\left(\sin^2\frac{2\pi l_c}{\lambda}\right)\Big/\left(\cos\frac{2\pi l_c}{\lambda} - 1\right)\right]\sin a_r\right]$$

so, using the relation $\sin^2 = 1 - \cos^2$

$$\left(\frac{\mathrm{d}V}{\mathrm{d}t}\right)_{\max} = -B_c H v \sin a_r = -B_c H v \sin a_r \tag{2.39}$$

where $(\mathrm{d}v/\mathrm{d}t)_{\max}$ is the maximum instantaneous wave pumping rate written as

$$a_r = -\pi l_c/\lambda$$

For instance, for the UK's SR.N5 hovercraft, in the case of $\lambda/2 = l_c = 9$ m, $H = 0.8$ m, $v = 35$ m/s then $(\mathrm{d}V/\mathrm{d}t)_{\max} \cong 150$ m^3/s, i.e. the maximum power due to the wave pumping is 172.7 kW. The total lift and propulsion power is 735 kW, of which about 30% or 221 kW is used to power the lift fan. It can be seen, therefore, that the lift system of SR.N5 can compensate the cushion flow rate consumed by the wave pumping motion at this speed.

2.7 Calculation of cushion stability derivatives and damping coefficients

In this section we will discuss the air cushion stability and hovering damping which are very important parameters concerning the longitudinal and vertical motion of ACVs hovering on a rigid surface. These parameters will greatly affect the natural heaving frequency, seaworthiness and comfort of craft, but are only relative to the static air cushion characteristics of ACVs. For this reason, these parameters are discussed in this chapter.

With respect to the SES, the air cushion stability and damping are also influenced by the buoyancy and damping force of sidewalls, because they are immersed in the water. The effect of sidewalls will be discussed at greater length in Chapter 9, though of course it is not difficult to derive them by means of the methods demonstrated in this chapter.

We take the ACV running over ground as an example and based on this the heaving motion can be illustrated in Fig. 2.24. $\dot{z}_c$ and $\dot{z}_e$ are heaving displacement and velocity respectively and z_e, $\dot{z}_e$, denote the motion amplitude and velocity of the ground plane, similar to the amplitude for waves.

The ACV can be described as an elastic system with a spring and damper connected parallel to each other. Strictly speaking, the spring and damping coefficients are nonlinear and asymmetric, i.e. they are rather different for upward and downward motion. As a first approximation, assuming vibration movement with minute displacement, the motion can be considered as approximately linear.

Thus an ACV running on a rough ground surface may be considered equivalent to

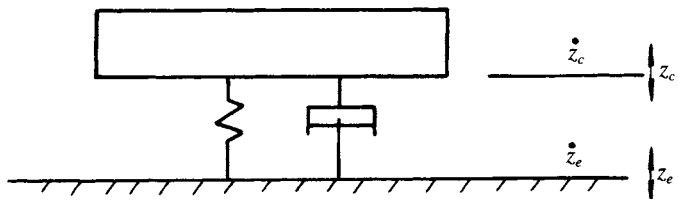

Fig. 2.24 Heave motion of a hovercraft model on rigid surfaces.

a vibration system with one degree of freedom (only the heaving motion is considered here) and the frequency response can be shown in Fig. 2.25, in which ω_e/ω_n denotes the tuning factor, ω_e represents the encounter frequency, namely the exciting frequency of ground relative to craft, ω_n is the natural vibration frequency, i.e. the heaving natural frequency of craft, and M represents magnification factor, i.e. the ratio of heave displacement to ground amplitude.

In Fig. 2.25, it can be seen that the higher the damping coefficient, the lower the magnification factor in the case where the tuning factor is close to 1. In the case of lower tuning factor, then higher damping coefficients give higher magnification factor. This means that the vertical motion of craft with a large damping coefficient will be violent in the case where the craft run in short waves or on a rough ground surface. Therefore the damping coefficient is very important for decreasing the vertical vibration of craft.

Before discussing these problems, we prefer to introduce three typical flow modes for craft in heaving motion as shown in Fig. 2.26: (a) shows equilibrium flow, i.e. static hovering mode of craft; (b) shows the flow underfed, i.e. the instantaneous skirt clearance will be smaller than the equilibrium skirt clearance as the craft drops down, consequently the jet flow cannot seal the cushion air causing some air leakage from the cushion; (c) shows the flow overfed, i.e. the instantaneous skirt clearance will be larger than the equilibrium skirt clearance as the craft lifts up, consequently more air flow will get into the cushion to fill up the air cavity. These three modes appear alternately as the craft heaves.

Calculation method for heaving stability derivatives and damping coefficients

First of all, the profile of the skirt is assumed unchangeable in the case of deriving the air cushion stability derivatives and damping coefficient. This assumption is

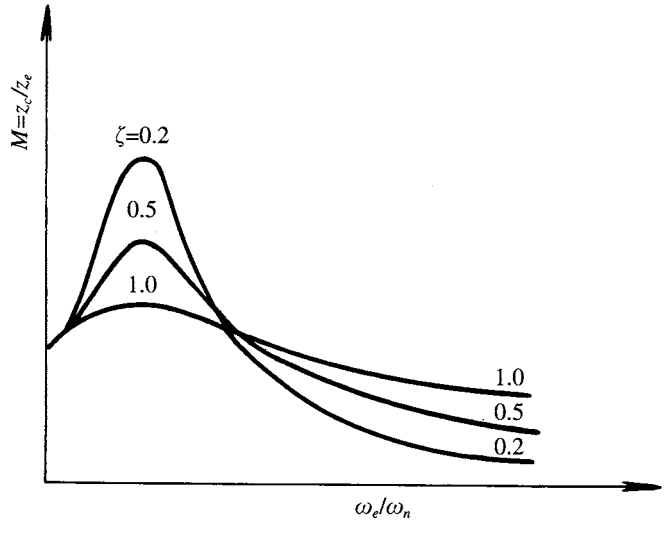

Fig. 2.25 Frequency response for heave motion with one degree of freedom.

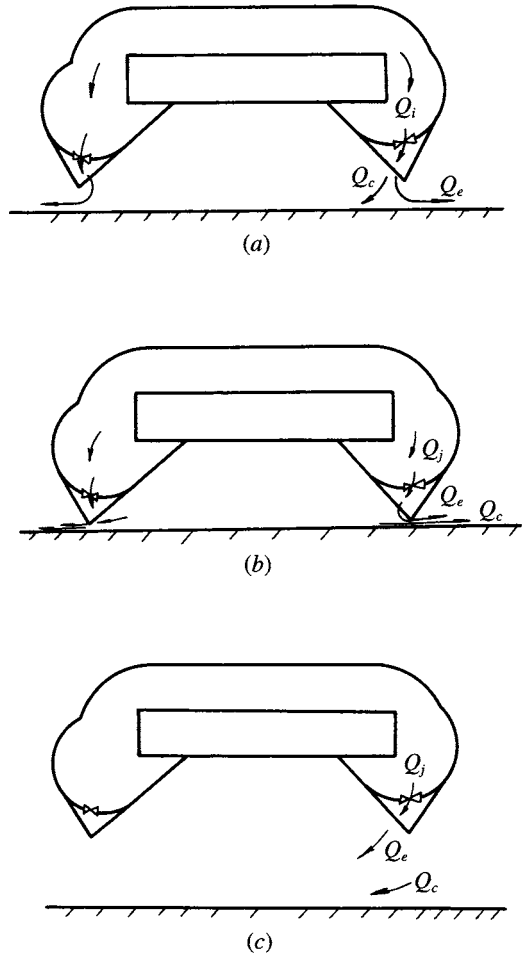

Fig. 2.26 Three conditions for heave motion of ACV: (a) equilibrium; (b) underfed; (c) overfed.

reasonable for a conventional medium pressure bag and finger type skirt for small perturbations. A responsive skirt with high deformability may have lower effective damping.

Regarding the effect of hovering performance and fan and air duct characteristics on the heaving stability and damping, we assume as follows:

1. The hovering performance of the skirt complies with the plenum chamber formula.
2. The flow air in the cushion is incompressible.
3. In order to compare the calculation value with experimental results, the rigid ground surface is considered to heave vertically, and we keep the craft hard structure unmovable.

Then, according to the flow continuity equation, we have

$$\frac{\mathrm{d}m}{\mathrm{d}t} = \rho_{\mathrm{a}}(Q_{\mathrm{i}} - Q_{\mathrm{o}}) = \frac{\mathrm{d}}{\mathrm{d}t}(\rho_{\mathrm{a}}V) = \rho_{\mathrm{a}}\frac{\mathrm{d}V}{\mathrm{d}t} + \frac{\mathrm{d}\rho_{\mathrm{a}}}{\mathrm{d}t} \tag{2.41}$$

where Q_o is the outflow rate from the cushion (m^3/s), Q_i the inflow rate into the cushion (m^3/s), V the cushion volume (m^3), m the mass of air in the cushion (Ns^2/m) and ρ_a the air density (Ns^2/m^4).

Considering the cushion as incompressible, thus $d\rho_a/dt = 0$. Then

$$Q_o = \psi A_t (2p_c/\rho_a)^{0.5}$$

where A_t is the area of air leakage (m). Now Q_i can be written as

$$Q_i = Q_{i0} + (\partial Q/\partial p_c)\, \Delta p_c$$

where $\Delta p_c = p_c - p_{c0}$, p_{c0} is the cushion pressure at equilibrium feed mode and p_c is the instantaneous cushion pressure.

If we assume that z, the displacement of the ground, is upward positive and there is no rotation of ground motion, then

$$dV/dt = -S_c \dot{z}$$

and

$$S_c = A_{i0} + (dA_i/dz)\, z = A_{i0} - lz$$

where S_c is the cushion area (m^2), A_{i0} the area of air leakage at equilibrium flow mode (m^2) and l the peripheral length for air leakage (m). Then substitute the foregoing equation into (2.41), which gives

$$-S_c \dot{z} = [Q_{i0} + (\partial Q/\partial p_c)\, \Delta p_c] - \psi (A_{i0} - z_1) \cdot (2p_c/\rho_a)^{0.5}$$

or

$$-S_c \dot{z} = Q_{i0} + (\partial Q/\partial p_c)\, \Delta p_c - \psi A_{i0} (2p_c/\rho_a)^{0.5} + \psi l_2 (2p_c/\rho_a)^{0.5}$$

Extend the $(2p_c/\rho_a)^{0.5}$ term into a Taylor series and neglect the nonlinear terms, and then these expressions can be written as

$$-S_c \dot{z} = Q_{i0} + \frac{\partial Q}{\partial p_c} \Delta p_c - \psi A_{i0} \left[\left(\frac{2p_{c0}}{\rho_a} \right)^{0.5} + \left(\frac{2}{\rho_a} \right)^{0.5} 0.5 \frac{\Delta p_c}{(p_{c0})^{0.5}} \right] + \psi l \left(\frac{2p_c}{\rho_a} \right)^{0.5} z$$

then

$$-S_c \dot{z} = Q_{i0} + \frac{\partial Q}{\partial p_c} \Delta p_c - Q_{i0} - \frac{Q_{i0}}{2p_{c0}} \Delta p_c + \psi l \left(\frac{2p_c}{\rho_a} \right)^{0.5} z \tag{2.42}$$

$$= \frac{\partial Q}{\partial p_c} \Delta p_c - \frac{Q_0}{2p_{c0}} \Delta p_c + \frac{Q_0}{h_0} z \tag{2.43}$$

where h_o is the skirt clearance at equilibrium flow mode (m), Q_{i0} the inflow rate at equilibrium flow mode (m^3/s) and p_{c0} the cushion pressure at equilibrium mode (N/m^2).

Equation (2.43) can be written as

$$K_1 \Delta p_c = -K_2 \dot{z} - K_3 z$$

or

$$\Delta p_c = \frac{-K_2}{K_1} \dot{z} - \frac{K_3}{K_1} z \tag{2.44}$$

where

$$K_1 = \frac{\partial Q}{\partial p_c} - \frac{Q_0}{2p_{c0}}$$

$$K_2 = S_c$$

$$K_3 = \psi l(2p_c/\rho_a)^{0.5} = Q_0/h_0 \tag{2.45}$$

Assume the cushion pressure is a linear function of heaving amplitude and velocity, then

$$\Delta p_c = \frac{\partial p_c}{\partial z}\dot{z} + \frac{\partial p_c}{\partial z}z \tag{2.46}$$

Using the equivalent terms of (2.46 and 2.44), we have

$$\frac{\partial p_c}{\partial \dot{z}} = -S_c\left[\frac{\partial Q}{\partial p_c} - \frac{Q_0}{2p_{c0}}\right] \tag{2.47}$$

$$\frac{\partial p_c}{\partial \dot{z}} = -(Q_0/h_0)\left[\frac{\partial Q}{\partial p_c} - \frac{Q_0}{2p_{c0}}\right] \tag{2.48}$$

where $\partial p_c/\partial \dot{z}$ is the velocity derivative of p_c with respect to z, i.e. the cushion damping coefficient, $\partial p_c/\partial z$ the derivative of p with respect to z, i.e. heaving stability derivatives and $\partial Q/\partial p_c$ the derivative of Q due to the characteristic curves of cushion air duct–fan systems with respect to p_c. Then

$$\frac{\partial Q}{\partial p_c} = \frac{\partial Q}{\partial H_j} \cdot \frac{\partial H_j}{\partial p_c} \cdot \frac{\partial p_t}{\partial p_c}$$

where $\partial Q/\partial H_j$ is the slope of the fan characteristic, if $H_j = A + BQ + CQ^2$, i.e.

$$\partial Q/\partial H_j = 1/(B + 2CQ)$$

$\partial H_j/\partial p_c$ is the slope of the air duct characteristic and $\partial p_t/\partial p_c$ the derivative of bag pressure with respect to cushion pressure, which can be calculated according to expression (2.3).

It is then not difficult to calculate the natural heave frequency without damping and heave damping rate:

$$\omega_z = \left[\frac{\partial p_c}{\partial z} \cdot \frac{S_c}{M}\right]^{0.5}$$

$$\zeta_z = \left[\frac{\partial p_c}{\partial \dot{z}} \cdot \frac{S_c}{2M\omega_z}\right] \tag{2.49}$$

where ω_z is the natural heave frequency without damping (s^{-1}), ζ_z the heaving damping rate and M the mass of the craft (kg).

Experimental methods for heave stability derivatives and damping coefficient

The foregoing formulae can be proved by experimental methods, in particular tests using ground excitation (a hinged base plate) in test skirt box equipment, then measuring the time history of cushion pressure, vertical displacement of the ground plate, total pressure of fans and flow rate, $z(t)$, $p_c(t)$, $H_j(t)$, $Q(t)$, as shown in Fig. 2.27.

Typical test equipment is shown in Fig. 2.6. This uses a 400 W electric motor via eccentric wheel to drive the ground plate in heaving motion. The heave amplitude $z(t)$ can be changed by changing the position of the eccentric wheel and a sliding linear resistance and potentiometer used to measure the time history of displacement of the ground plate.

The ground plate will move in simple harmonic motion, i.e. the eccentric wheel moves in circular motion with constant angular velocity. For this reason the variables $p_c(t)$, $H_j(t)$, $Q(t)$, are also in simple harmonic motion. $H_j(t)$ and $p_c(t)$ can be measured by capacitance type pressure sensors.

The following physical phenomena can be observed during such tests:

- The fluctuation of fan total pressure is small.
- As shown in Fig. 2.27, the cushion flow forms underfed mode as the ground platform is moved upward, i.e. the points B, C denote underfed and points D, A denote overfed flow mode with p dropping down.
- As shown in Fig. 2.27, the $p_c(t)$ precedes the $z(t)$ and the phase lead is ε. Heave velocity equals zero at points A and C and the heaving velocity reaches maximum heave displacement equal to zero at points B and D.

Then the stability coefficient and damping coefficient can be written as

$$-\partial p_c/\partial h = \partial p_c/\partial z = -\Delta p_{cA}/z_m = \Delta p_{cC}/z_m \tag{2.50}$$

$$-\partial p_c/\partial h = \Delta p_{cB}/\omega z_m = -\Delta p_{cD}/\omega z_m \tag{2.51}$$

B and D denote the maximum heaving velocity, while A and C are the maximum heaving displacement z. In addition because of simple harmonic motion in heave, z can be written as

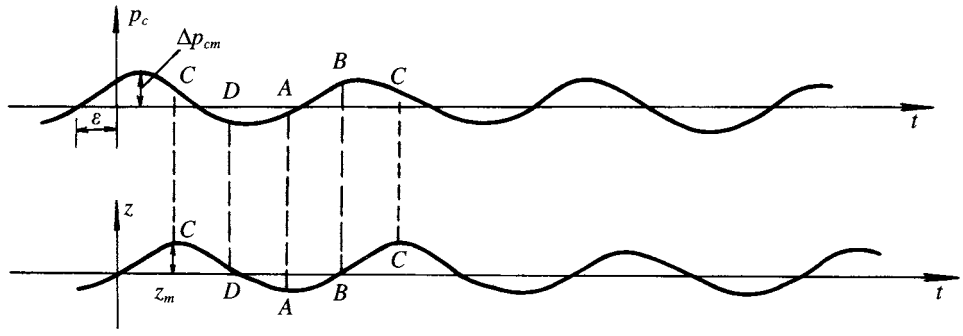

Fig. 2.27 Time history of cushion pressure and heave amplitude.

$$
\begin{aligned}
z &= z_m \sin \omega_t \\
\Delta p_c &= \Delta p_{cm} \sin(\omega t + \varepsilon) \\
&= \Delta p_{cm} \sin \omega t \cos \varepsilon + \Delta p_{cm} \cos \omega t \sin \varepsilon
\end{aligned} \tag{2.52}
$$

and

$$
\begin{aligned}
\Delta p_c &= \frac{\partial p_c}{\partial z} \cdot z + \frac{\partial p}{\partial \dot{z}} \cdot \dot{z} \\
&= \frac{\partial p_c}{\partial z} \cdot z_m \sin \omega t + \frac{\partial p}{\partial \dot{z}} \cdot z_m \omega \cos \omega t
\end{aligned} \tag{2.53}
$$

then

$$
\begin{aligned}
\frac{\partial p}{\partial \dot{z}} &= \frac{\Delta p_{cm} \sin \varepsilon}{z_m \omega} \\
\frac{\partial p}{\partial z} &= \frac{\Delta p_{cm} \cos \varepsilon}{z_m}
\end{aligned} \tag{2.54}
$$

The stability and damping coefficient can then be obtained using equations (2.50), (2.51) and (2.54) from measurements taken on the rig using known values.

Comparison of calculations with test results

1. A comparison of calculations with test results is shown in Figs 2.28 and 2.29 and it is found that the calculated values are in good agreement. The latter are higher than the former, because of the air leakage from the connecting parts of the flexible skirts (the results are uncorrected). The flow in test is consequently larger than the actual value, and the calculation values are smaller than the test results.
2. From equation (2.47), it is found that because $\partial Q/\partial p_c < 0$ and both $Q_0 > 0$ and $p_c > 0$, this means that the steeper the fan characteristic curve (H_j–Q), the smaller $\partial Q/\partial H_j$ and the larger the damping coefficient.
3. From the formulae, one can see that the heave stability is proportional to flow rate and inversely proportional to skirt clearance; and that the relation between the heave stability and the characteristic curve of fan/air ducting is similar to the relation between the damping coefficient and the characteristic of fan/air ducting, namely that mentioned in (2) above.

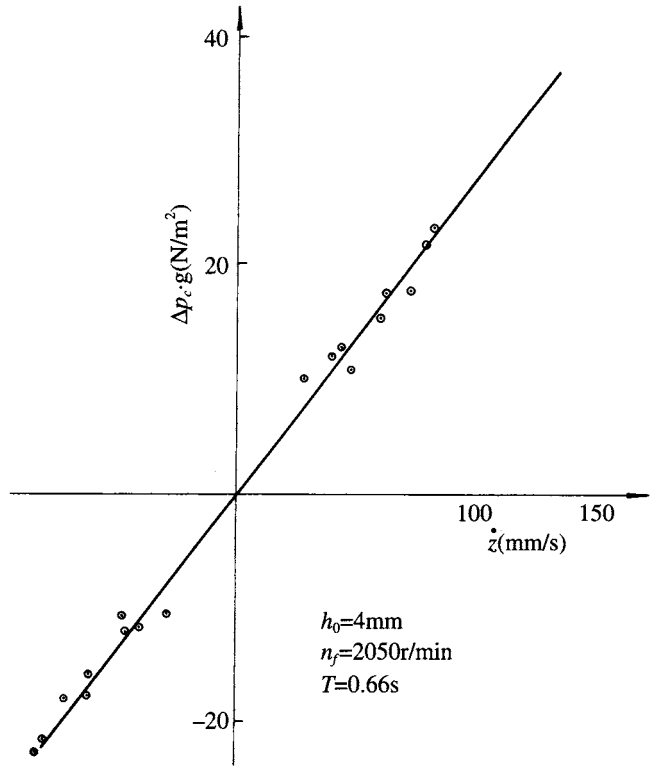

Fig. 2.28 Comparison of p_c between the calculated and experimental result as a function of heaving velocity.

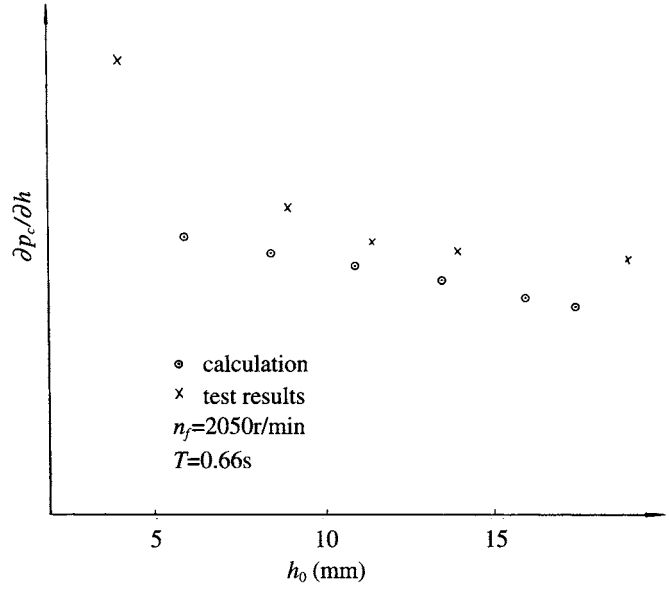

Fig. 2.29 Comparison of heave position derivative between calculations and measurements as a function of air gap.